Green Chemistry

PAPER

View Article Online
View Journal | View Issue

Cite this: *Green Chem.*, 2018, **20**, 5327

Noble metal-free upgrading of multi-unsaturated biomass derivatives at room temperature: silyl species enable reactivity†

Hu Li,[a] Wenfeng Zhao,[a] Wenshuai Dai,[b] Jingxuan Long,[a] Masaru Watanabe,[c] Sebastian Meier,*[d] Shunmugavel Saravanamurugan,*[e] Song Yang*[a] and Anders Riisager[d]

Received 16th September 2018,
Accepted 26th October 2018

DOI: 10.1039/c8gc02934b

rsc.li/greenchem

Biomass derivatives are a class of oxygen-rich organic compounds, which can be selectively upgraded to various value-added molecules by partial or complete hydrogenation over metal catalysts. Here, we show that Cs_2CO_3, a low-cost commercial chemical, enables the selective reduction of dicarbonyl compounds including bio-derived carboxides to monohydric esters/amides, hydroxylamines or diols with high yields (82–99%) at room temperature using eco-friendly and equivalent hydrosilane as a hydride donor. The *in situ* formation of silyl ether enables the developed catalytic system to tolerate other unsaturated groups and permits a wide substrate scope with high selectivities. Spectroscopic and computational studies elucidate reaction pathways with an emphasis on the role of endogenous siloxane.

Introduction

Catalytic hydrogenation of unsaturated carbon-containing bonds (C=C, C=N, and C=O) in organic compounds with metal complexes or particles is a prolific approach that is extensively applied in the petroleum, pharmaceutical, fine chemical, perfume and flavoring industries.[1] Noble (*e.g.*, Au, Pt, Ru, and Rh) and transition (*e.g.*, Fe, Co, Ni, and Cu) metals prevail in both heterogeneous and homogeneous catalytic hydrogenation processes as catalysts with favourable activity and selectivity.[2] The co-use of unique organic/inorganic ligands, suitable acidic species, or additional metallic additives with relatively harsh reaction conditions is a prerequisite to ensure good reactivity in the hydrogenation process, which on the other hand may lead to accelerated catalyst deactivation.[3]

Currently, much attention is being paid to the selective hydrogenation of unsaturated functionalities. For example, partial or complete reduction of oxygenates to alcohols or alkanes,[4] regioselective reduction of polyols or polyenes,[5] and selective hydrogenation of α,β-unsaturated carbonyl compounds[6] can be achieved using well-designed metal catalysts. Given the significance of selectivity in reduction reactions, it would be especially attractive to control the hydrogenation capability toward multi-unsaturated functional groups with similar redox potentials. As the most abundant organic carbon source derived from photosynthesis, lignocellulosic biomass has been explored as promising renewable feedstock for producing a wide range of platform molecules that can compete with petroleum-based products.[7] One of the bottlenecks for the efficient upgrading of biomass is the selective hydrogenation of oxygenated species that are rich in downstream derivatives such as sugar, organic acids, and aromatic and furanic carbonyl compounds,[8] especially those concurrently containing two or more different types of carbonyl groups. Levulinic acid (LA) and its esters are a class of biomass-derived dicarbonyl compounds,[9] which can be selectively hydrogenated to value-added products, especially γ-valerolactone (GVL) and 1,4-pentanediol (1,4-PD) over metal catalysts.[10] Significant progress has been achieved with metal-mediated biomass valorisation processes in the presence of excessive hydrogen donors along with high pressure and reaction temperature (Table S1†), while the development of more benign and cost-effective catalytic systems would be desirable.

[a]*State Key Laboratory Breeding Base of Green Pesticide & Agricultural Bioengineering, Key Laboratory of Green Pesticide & Agricultural Bioengineering, Ministry of Education, State-Local Joint Engineering Lab for Comprehensive Utilization of Biomass, Center for R&D of Fine Chemicals, Guizhou University, Guiyang, Guizhou 550025, China. E-mail: jhzx.msm@gmail.com*
[b]*Beijing National Laboratory of Molecular Science, State Key Laboratory of Molecular Reaction Dynamics, Institute of Chemistry, Chinese Academy of Sciences; University of Chinese Academy of Sciences, Beijing 100049, China*
[c]*Research Center of Supercritical Fluid Technology, Graduate School of Engineering, Tohoku University, 6-6-11, Aoba, Aramaki, Aoba-ku, Sendai 980-8579, Japan*
[d]*Department of Chemistry, Technical University of Denmark, DK-2800 Kgs. Lyngby, Denmark. E-mail: semei@kemi.dtu.dk*
[e]*Laboratory of Bioproduct Chemistry, Center of Innovative and Applied Bioprocessing (CIAB), Mohali 140 306, Punjab, India. E-mail: saravana@ciab.res.in*
†Electronic supplementary information (ESI) available. See DOI: 10.1039/c8gc02934b

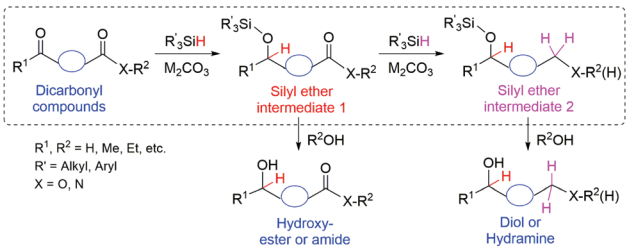

Fig. 1 Selective hydrogenation of dicarbonyl compounds to hydroxy-ester/amide or diol/hydramine catalysed by alkali carbonates (M_2CO_3).

In most cases, precious or transition metal species coupled with suitable additives have been reported to be efficient catalysts for the hydrogenation reactions.[11] Due to significantly enhanced sustainability, alkali carbonates, which are low-cost, pollution-free and obtainable from CO_2,[12] seem to be better candidates for the hydrogenation reactions. In the present study, we present a sustainable carbonate-based catalytic process (Fig. 1) that is able to selectively hydrogenate dicarbonyl compounds and tolerate other unsaturated moieties by using environmentally benign, cheap, and air-stable hydrosilanes[13] as a hydride source. The silyl ether species formed *in situ* in the hydrogenation process enable the control of selectivity in the reduction of multi-unsaturated carbonyl compounds that bear aldehyde/ketone, ester/amide, and aromatic/furanic groups.

Results and discussion

Controllable hydrogenation of bio-based ethyl levulinate

Initial screening studies were conducted to investigate the selective hydrogenation of ethyl levulinate (EL) to GVL or 1,4-PD over Cs_2CO_3 using triethoxysilane $(EtO)_3SiH$ as a reducing agent in the biomass-derived solvent 2-methyltetrahydrofuran (MTHF), and the results are shown in Table 1. At room temperature (25 °C) in the presence of Cs_2CO_3 and 1.5 equiv. H^-, 74% yield of GVL could be achieved from EL in 0.5 h, while the silyl ether **Si-1** (21%) was found to be the dominant byproduct (Table S2,† entry 1). After treatment with ethanol under stirring at 25 °C for 2 h, the GVL yield increased to 87% by partial consumption of **Si-1** (10% yield; Table S2,† entry 2). Upon further increase of the post-treatment temperature to 80 °C, a high GVL yield of 98% was obtained with a TOF value of 39.2 h^{-1} (Table 1, entry 1), giving tetraethyl orthosilicate $[Si(OEt)_4]$ as the co-product (Fig. S1 and S2†).

In addition to Cs_2CO_3, other alkali carbonates including K_2CO_3, Na_2CO_3, and Li_2CO_3 were examined and were proved to be almost inactive for the hydrogenation of EL with no more than 2% conversion (Table S2,† entries 3–5). This finding seems to imply a positive role of cesium in the hydrogenation process. However, the inactivity of CsCl, $CsNO_3$ and CsOOCH (Table S2,† entries 6–8) is contradictory to the speculation, which on the other hand indicates the activation effect of the carbonate. The co-addition of 18-crown-6 (10 mol%) signifi-

Table 1 Selective hydrogenation of ethyl levulinate (EL) to γ-valerolactone (GVL) and 1,4-pentanediol (1,4-PD) *via* silyl ethers (**Si-1** and **Si-2**)

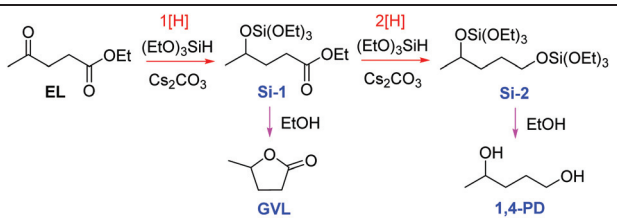

Entry	Catalyst	Hydrogen-donor		Temp. (°C)	Time (h)	EL conv. (%)	Product yield (%)				CB[a] (%)	TOF[b] (h^{-1})
		Type	H^- dosage				**Si-1**	GVL	**Si-2**	1,4-PD		
1	Cs_2CO_3	$(EtO)_3SiH$	1.5 equiv.	25	0.5	>99	<1	98	<1	0	99	39.2
2	CsOH	$(EtO)_3SiH$	1.5 equiv.	25	0.5	100	0	82	2	13	97	32.8
3	Cs_2CO_3	$(EtO)_3SiH$	3.5 equiv.	25	0.5	100	0	92	3	4	99	36.8
4	CsOH	$(EtO)_3SiH$	3.5 equiv.	25	0.5	100	0	51	<1	38	89	20.4
5	Cs_2CO_3	$(EtO)_3SiH$	3.5 equiv.	25	2	100	0	77	1	20	98	7.7
6	Cs_2CO_3	$PhSiH_3$	3.5 equiv.	25	0.5	99	<1	72	1	25	>99	28.8
7	Cs_2CO_3	$PhSiH_3$	3.5 equiv.	25	6	100	0	2	<1	95	97	3.2
8	Cs_2CO_3	$PhSiH_3$	3.5 equiv.	60	2.5	100	0	<1	0	87	87	6.9
9[c]	Pt/V_2O_5	5 MPa H_2	—	130	6	>99	—	99	—	1	100	16.5
10[c]	Pt-Mo/HAP	3 MPa H_2	—	130	24	>99	—	<1	—	93	94	1.9
11[d]	$Pt-Mo/SiO_2$	5 MPa H_2	—	130	24	>99	—	0	—	48	93	1.0
12[e]	CuAlZn	4 MPa H_2	—	160	10	100	—	17	—	82.9	99.9	0.1
13[f]	Cs_2CO_3	$(EtO)_3SiH$	1.5 equiv.	25	0.5	95	0	93	<1	0	98	37.2
14[g]	Cs_2CO_3	PMHS	1.5 equiv.	25	2	96	<1	90	<1	2	97	9.0

Reaction conditions: 1 mmol EL, 1.5 or 3.5 equiv. H^-, 5 mol% catalyst, 2 mL MTHF; after the reaction, 2 mL ethanol was added into the reaction mixture and stirred at 80 °C for 2 h. [a] CB: Carbon balance. [b] TOF (turnover frequency) is defined as (moles of the primary product)/(moles of active species × time). [c] Ref. 14*a*. [d] Ref. 14*b*. [e] Ref. 14*b*. [f] LA instead of EL was used as the substrate. [g] Polymethylhydrosiloxane (PMHS) was used as a reducing agent.

cantly enhanced the performance of K_2CO_3 in the reaction (Table S2,† entry 9) by increasing its solubility, clearly proving the dominant role of the carbonate in the catalytic process. Although CsOH showed comparable activity to Cs_2CO_3 in terms of EL conversion, the selectivity toward GVL significantly dropped to 82% with 1,4-PD as the primary byproduct (13% yield; Table 1, entry 2). This result further indicates that the appropriate nucleophilicity of the dissociative carbonate is crucial for the pronounced reactivity in the selective hydrogenation of the dicarbonyl compound. In line with this finding, the type of solvent was illustrated to significantly influence the reactivity (Fig. S3†), where MTHF is capable of dispersing Cs_2CO_3 and $(EtO)_3SiH$ to enable their contact with the substrate EL. In contrast, more polar solvents (DMSO and acetonitrile) were not able to completely convert EL (Fig. S3†), while a less polar solvent (*n*-hexane) promoted the over-hydrogenation of GVL to afford the corresponding acetal and 1,4-PD (Fig. S4 and S5†). In the case of using tetrahydrofuran (THF) as the solvent with a structure quite similar to that of MTHF, GVL was found to be the predominant product after post-treatment at variable temperatures (Fig. S6†), while GVL-derived acetals (2-ethoxy-5-methyltetrahydrofuran and triethyl (5-methyltetrahydrofuran-2-yl) silicate) without 1,4-PD and MTHF were detected by GC-MS (Fig. S7†).

Both the type and dosage of hydrosilanes were found to directly affect both EL conversion and selectivity towards GVL or 1,4-PD. Among the tested hydrosilanes, $(EtO)_3SiH$ exhibited the highest activity in the synthesis of GVL from EL, while the other hydrosilanes were either too active (with *ca.* 9% yield of 1,4-PD obtained in the presence of $PhSiH_3$) or inert (*e.g.*, Et_3SiH and Ph_2SiH_2) for the reaction (Table S3†). 1.5 equiv. H^- of $(EtO)_3SiH$ were most favorable for the formation of GVL (Fig. S8†), while the use of a larger excess of hydrosilane (2.5–5.5 equiv. H^-) resulted in the reduction of the ester group in either EL or GVL (Fig. S1†), giving 1,4-PD as the major co-product in up to *ca.* 10% yield. Owing to its relatively low nucleophilicity, Cs_2CO_3 showed inferior activity relative to CsOH in the formation of 1,4-PD (yield: 4% *vs.* 38%; Table 1, entries 3 and 4). However, a low carbon balance was observed in the latter case (89%), which could be ascribed to the presence of strongly basic OH^- causing undesired side reactions like condensation or the formation of stable intermediates such as 2-ethoxy-5-methyltetrahydrofuran (Fig. S9†). It should be noted that an increased 1,4-PD yield of 71% with 21% GVL could be obtained with Cs_2CO_3 and 3.5 equiv. H^- of $(EtO)_3SiH$ by prolonging the reaction time to 6 h (Fig. S10†). When the more active phenylsilane ($PhSiH_3$) was used as a reducing agent in the presence of Cs_2CO_3, a 25% yield of 1,4-PD was obtained after 0.5 h, which is comparable to the yield (20%) achieved with $(EtO)_3SiH$ after 2 h under otherwise identical conditions (Table 1, entries 5 and 6). With an extension of the reaction time to 6 h, an unprecedented high yield of 1,4-PD (95%) was attained using Cs_2CO_3 and $PhSiH_3$ (Table 1, entry 7). Although a slight increase of the reaction temperature to 60 °C enhanced the reaction rate from 3.2 to 6.9 h^{-1}, the 1,4-PD yield together with the carbon balance was markedly reduced to *ca.* 87% (Table 1, entry 8), due to the formation of some unidentified products. These results demonstrate that room temperature (25 °C) was preferable to warrant high carbon balance through the reaction process, while the dosage and type of hydrosilane as well as the reaction time were key factors determining the selectivity and product distribution.

For comparison, some previously reported results using metal-based catalysts for the production of GVL and 1,4-PD are listed in Table 1, entries 9–12.[14] The Pt/V_2O_5 catalyst could afford a yield of GVL (99%) comparable to our catalytic system (entry 9 *vs.* entry 1), but harsher reaction conditions (130 °C, 6 h, and 5 MPa H_2) were required and the reaction rate was much lower (TOF: 16.5 h^{-1} with Pt/V_2O_5 *vs.* 39.2 h^{-1} with Cs_2CO_3 at 25 °C). Even higher reaction temperature (160 °C), longer reaction time (10–24 h), or higher H_2 pressure (3–5 MPa) was required over metallic catalysts to produce 1,2-PD with yields of 48–93% and TOF values of 0.1–1.9 h^{-1} (entries 10–12). It is also worth noting that the metal catalysts with serious leaching and toxicity issues are prone to cause the formation of a cyclic ether or mono-alcohol. For example, MTHF (19%), 2-pentanol (20%), and 1-pentanol (6%) were found to be the major byproducts using $Pt\text{-}Mo/SiO_2$ (39), thus greatly annihilating the selectivity toward 1,4-PD (48%; entry 11). In contrast, our catalytic system was able to selectively produce 1,4-PD in a higher yield of 95% with a TOF value of 3.2 h^{-1} (entry 7) by simply increasing the hydrosilane dosage from 1.5 to 3.5 equiv. of H^-. This finding manifests the advantages of the Cs_2CO_3-promoted hydrosilylation process in the selective hydrogenation of EL, a dicarbonyl compound, into GVL or 1,4-PD at room temperature.

Interestingly, when LA instead of EL was used as a substrate, a good GVL yield of 93% (Table 1, entry 13) was also obtained under the optimal reaction conditions, indicating that the developed catalytic system can be potentially used for the reduction of biomass-derived organic acids. As one of the promising silanes used for hydrogenation, polymethylhydrosiloxane (PMHS) is a polymeric byproduct of the silicone industry, which is non-toxic, inexpensive, safe, and water/air insensitive.[15] Although a low GVL yield (25%) was obtained using PMHS after a short reaction time of 0.5 h (Table S3†), the yield could be improved to *ca.* 90% over our developed catalytic system by prolonging the reaction time to 2 h (Table 1, entry 14). In order to examine the feasibility of the developed catalytic system in practical production, the reaction was scaled up from 2 to 50 mL, and the amount of EL was accordingly increased from 144 mg to 3.6 g. Although the substrate was scaled up from milligram to gram by 25-fold, GVL and 1,4-PD could be obtained in good yields of 90 and 82% with 5 mol% Cs_2CO_3 at 25 °C using 1.5 equiv. H^- of $(EtO)_3SiH$ and 3.5 equiv. H^- of $PhSiH_3$ after 1 h and 8 h, respectively. These results demonstrate the great potential of the Cs_2CO_3–hydrosilane catalytic system for industrial applications.

NMR study of reaction pathways

To elucidate the reaction pathways, *in situ* NMR studies were conducted to monitor the product distribution during the

reduction process of EL to GVL in the presence of Cs_2CO_3 with $(EtO)_3SiH$. The *in situ* ^{13}C NMR spectra of the EL hydrogenation (Fig. 2A) display that silyl ether (**Si-1**) and ethyl 4-hydroxypentanoate (EHP) are possibly key intermediates to the final product GVL. EL was almost completely converted in 0.5 h even without magnetic stirring, where **Si-1** was observed as the first intermediate, followed by gradual degradation to EHP (Fig. S11†). On the other hand, the absence of signals in the olefinic region in the *in situ* ^{13}C NMR spectra of the reaction mixture (Fig. 2B) validates the initial occurrence of the hydrogenation step, rather than a possible initial cyclization of EL to form α-angelica lactone (Fig. 3). After the reaction for different intervals (3–60 min), the characteristic regions belonging to EHP and GVL in *ex situ* NMR spectra of the reaction mixture quenched by methanol were recorded (Fig. S12†). Clearly, better selectivity toward GVL was observed after methanol treatment, as compared with the *in situ* obtained results (Fig. 2A) in the NMR tube. This finding verifies the importance of the post-treatment process (*e.g.*, with ethanol) at the specific

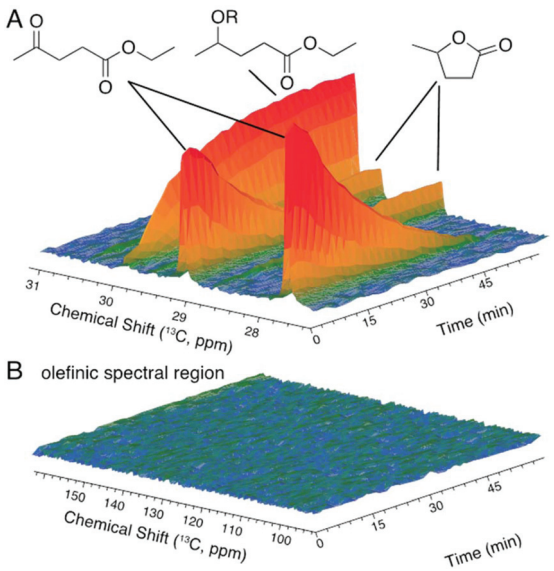

Fig. 2 *In situ* ^{13}C NMR spectra for the hydrogenation of ethyl levulinate (EL). (A) Formation of γ-valerolactone (GVL) *via* the silyl ether (**Si-1**) and ethyl 4-hydroxypentanoate (EHP); (B) olefinic region in ^{13}C NMR spectra of the reaction mixture. Reaction conditions: 1 mmol EL, 1.5 equiv. H^- of $(EtO)_3SiH$, 5 mol% Cs_2CO_3, 2 mL MTHF, 25 °C.

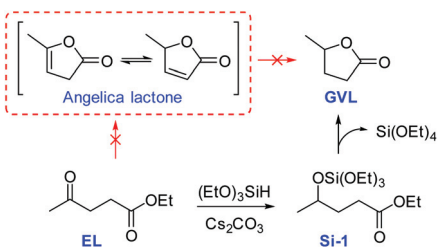

Fig. 3 Reaction pathway for EL-to-GVL conversion.

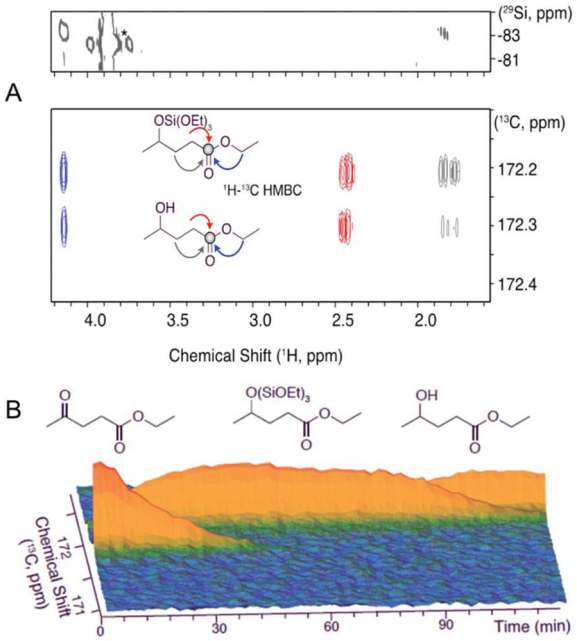

Fig. 4 *In situ* NMR spectra of the reaction mixture for ethyl levulinate (EL) conversion. (A) *In situ* $^1H-^{13}C/^{29}Si$ HMBC spectra of the intermediates [ethyl 4-hydroxypentanoate (EHP) and silyl ether (**Si-1**)], and (B) *in situ* time-series of ^{13}C NMR spectra for the hydrogenation of ethyl levulinate (EL) to the intermediates [silyl ether (**Si-1**) and ethyl 4-hydroxypentanoate (EHP)]; tetraethyl orthosilicate is indicated by the asterisk in the $^1H-^{29}Si$ HMBC spectrum (top).

temperature (*ca.* 80 °C) to accomplish the following cyclization step, thus exclusively yielding GVL.

The simultaneous presence of the intermediates EHP and **Si-1** in the reaction mixture can also be distinguished by the $^1H-^{13}C$ HMBC spectra of the reaction mixture (Fig. 4A). The Si attachment in **Si-1** can be affirmed by $^1H-^{29}Si$ HMBC (Fig. 4A). To some extent, the stable intermediates are not favorable for directly producing GVL from EL, due to the requirement of secondary post-treatment. Fortunately, the reaction rate is significantly enhanced after a specific period (*ca.* 15–30 min) of the steady reaction process, as shown in Fig. 4B. The formation of the intermediates and the siloxane $Si(OEt)_4$ most likely promotes the dissolution of the catalytically active species (carbonate), thus leading to a rapid or runaway reaction. Furthermore, the incorporation of the hydride from the hydrosilane into the substrate EL can be illustrated by a comparison of the obtained ^1H NMR spectra (Fig. S13†) using normal Ph_2SiH_2 and deuterium-labeled Ph_2SiD_2 as reducing agents. A kinetic isotope effect (KIE) study disclosed a significant difference in the k_H/k_D value (*ca.* 2.4) when the hydride was supplied either by Ph_2SiH_2 or Ph_2SiD_2, further supporting the fact that the relative activity of the employed hydrosilane plays a key role in the selective hydrogenation. On the other hand, $^1H-^{13}C$ HSQC NMR spectra of the reaction mixture after post-treatment with methanol-d_4 at 60 °C for 2 h demonstrated the complete conversion of the intermediates into GVL (Fig. S14†),

which is in agreement with the corresponding ^{13}C NMR spectra (Fig. S15 and S16†).

Upgrading of the carbonate

Although the used catalyst Cs_2CO_3 is cheap, widely available and eco-friendly, attempts were made to investigate its recoverability for potential recycling or further upgrading. Initially, the effect of Cs_2CO_3 dosage on the conversion of EL to GVL was studied, where no more than 80% yield of GVL was obtained using less than 5 mol% Cs_2CO_3 (Fig. S17†). This relatively low yield shows the importance of using sufficient Cs_2CO_3 (5 mol%) for good catalytic performance. However, the amount of Cs_2CO_3 (separated out by centrifugation) was decreased by around 68% after the first cycle of the reaction. Notably, the recovered solids were characterized by STEM (Fig. S18†) to be Cs_2CO_3 with additional silicon compounds, thus underlining the difficulty in completely recycling the catalyst. TEM images of both fresh and recovered Cs_2CO_3 pre-dispersed into THF indicated the formation of nano-sized particles (Fig. S19†), which is in agreement with the superior catalytic results of the alkali carbonate salts which are more soluble (Table S2,† entries 1–5). Instead, the addition of ethanol (2 mL) into the liquid mixture after the reaction led to full conversion of the residual carbonate in both solid and leached states into the formate (>95% yields) in 2 h (Fig. S20†), which was confirmed by ^1H NMR through the detection of a singlet with a chemical shift of about 8.6 ppm belonging to $^1HCOO–$ (Fig. S21†). Therefore, it would be more preferable to co-synthesize the expected products together with the value-added formate by post-treatment with ethanol.

Selective hydrogenation of dicarbonyl compounds to hydroxy esters and diols

Cyclic ether or mono-alcohol is typically formed in the synthesis of diols from dicarbonyl compounds.[14b,16] To examine the versatility of the catalytic system developed in this study, the substrate scope was further expanded to other dicarbonyl compounds (Table 2). Both diketones and dialdehydes could be selectively reduced to diols with yields of 87–95% in 0.5–1 h (entries 1–3). The exclusive selectivity toward the diols further indicates the intact C–O bond during the processes of reduction and post-treatment, which is unambiguously attributed to the formation of silyl ether under the mild reaction conditions. Apart from the aromatic ring, the nitro group was also intact during the hydrogenation process (entry 4). This makes the catalytic system capable of exclusively producing alcohols with good compatibility with other multi-unsaturated functional groups. By prolonging the reaction time to 6 h and increasing the hydrosilane dosage to 2.5 equiv. H^- of $PhSiH_3$, methyl benzoate and methyl *p*-methyl benzoate could be hydrogenated to benzyl alcohol (96% yield, entry 5) and *p*-methylbenzyl alcohol (>99% yield, entry 6), respectively. In the presence of both aldehyde/ketone and ester, the selective reduction of the aldehyde or ketone to an alcohol without affecting the ester group could be achieved (entries 7, 9 and 11). Importantly, both the presented carboxides could be reduced to diols in high yields of 88–96% from these dicarbonyl compounds containing aldehyde/ketone and ester groups (entries 8, 10 and 12).

Table 2 Selective reduction of carbonyl compounds bearing multi-unsaturated groups to alcohols *via* silyl ethers

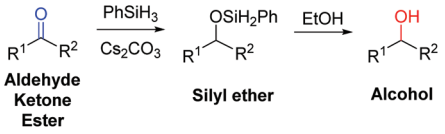

Entry	Substrate	Hydride (H^- equiv.)	Time (h)	Alcohol yield (%)
1		2.5	1	92
2	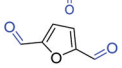	2.5	1	87
3	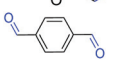	2.5	1	95
4	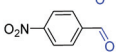	2.5	1.5	97
5	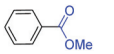	2.5	6	96
6	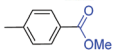	2.5	12	>99
7	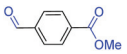	1.5	0.5	98
8		3.5	24	96
9	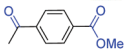	1.5	1	94
10		3.5	24	91
11	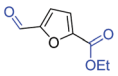	1.5	1	85
12		3.5	24	88

Reaction conditions: 1 mmol substrate, 1.5–3.5 equiv. H^- of $PhSiH_3$, 5 mol% Cs_2CO_3, 2 mL MTHF, 25 °C; after the reaction, 2 mL ethanol was added to the liquid mixture and stirred at 80 °C for 2 h.

Selective hydrogenation of multi-unsaturated amides

Pyrrolidones are a class of amides extensively applied as solvents and feedstocks for fibers or surfactants.[17] In the present study, starting from levulinic acid (LA) and amines, a variety of *N*-substituted lactams (*i.e.*, pyrrolidones) could be synthesized in good yields of 85–92% at 120 °C using formic acid both as an acid and as a hydrogen source in the absence of a catalyst (Table S4†). The results are comparable to those obtained over metal catalysts such as Ir and Ni in the production of lactams.[17,18] In general, the controllable reduction of lactams is one of the promising ways to produce cyclamines. However, the cleavage of C–N bonds often occurs over metal (*e.g.*, Ru, Mn, and Fe) catalysts during the hydrogenation process, simultaneously giving amines and alcohols as products.[19] Typically, the lactam is more inert towards reduction compared with the ester analogue,[11e] while the extension of the reaction time to 24–36 h could yield 81–99% cyclamine with a selectivity of 95–100% in the presence of the hydrosilane/Cs_2CO_3 catalytic system at room temperature (Table 3). Notably, this catalytic system is compatible with aliphatic and aromatic *N*-substituents, and it does not interfere with the halogen substituent resulting in the hydrodechlorination reaction.

Table 3 Selective hydrogenation of *N*-substituted lactams derived from levulinic acid

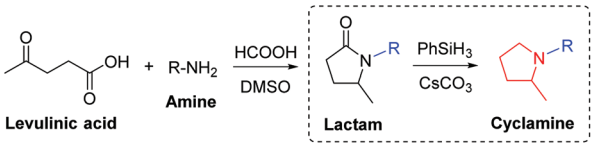

Entry	Lactam	Time (h)	Cyclamine (%) Yield	Selectivity
1	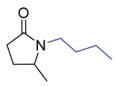	24	92	97
2	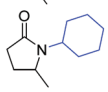	36	81	95
3	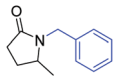	36	99	100
4	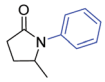	36	85	96
5	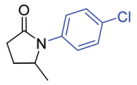	24	93	98

Reaction conditions: 1 mmol substrate, 3 equiv. H^- of $PhSiH_3$, 5 mol% Cs_2CO_3, 2 mL MTHF, 25 °C; after the reaction, 2 mL ethanol was added to the reaction mixture and stirred at 80 °C for 2 h.

Table 4 Selective reduction of amides bearing other unsaturated groups to cyclic amines

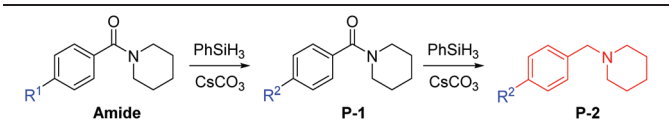

Entry	R^1	R^2	Hydride (equiv.)	Time (h)	Yield (%) **P-1**	**P-2**
1	-CHO	$-CH_2OH$	1.5	1	97	<1
2		$-CH_2OH$	4.5	24(6)[a]	<1	93(95)[a]
3			1.5	2	94	<1
4			4.5	30(8)[a]	<1	87(92)[a]
5	$-NO_2$	$-NO_2$	3	24	1	90
6	-CN	-CN	3	24	2	82

Reaction conditions: 1 mmol substrate, 1.5–4.5 equiv. H^- of $PhSiH_3$, 5 mol% Cs_2CO_3, 2 mL MTHF, 25 °C; after the reaction, 2 mL ethanol was added into the reaction mixture and stirred at 80 °C for 2 h. [a] Data in the parentheses were obtained at 60 °C under otherwise identical conditions.

With respect to the amides bearing multi-unsaturated groups, the substrate scope was also investigated at 25 °C for the selective hydrogenation (Table 4). Either the aldehyde or ketone could be hydrogenated to an alcohol with yields of 97 or 94% in 1 or 2 h, respectively (entries 1 and 3), while the amide remained almost unreacted (<1%). After reacting for 24 or 30 h with 4.5 equiv. H^- of $PhSiH_3$, the hydrogenation of the amide to amine proceeded giving hydramine in ~90% yield (entries 2 and 4). This finding indicates that the initial reduction of aldehydes or ketones to the corresponding silyl ethers was kinetically favorable and proceeded to completion relatively rapidly. On the other hand, the hydrogenation of the amide group was most likely thermodynamically controlled, where an increase of the reaction temperature from 25 to 60 °C significantly shortened the reaction time from 24–30 h to 6–8 h with comparable hydramine yields (entries 2 and 4). Even in the presence of other unsaturated functional groups (*e.g.*, $-NO_2$ and –CN), the amide compounds were selectively reduced at room temperature (entries 5 and 6), leaving the other functional groups intact. This unprecedented selectivity toward hydrogenates shows great potential in the controllable reduction of multi-unsaturated carbonyl compounds. Thus, the reaction system permits the selective reduction of amides under mild conditions, which is an enduring challenge in pharmaceutical processes.[20] Overall, the chemistries described herein thus have the potential to impact on the upgrading of biomass-derived chemicals and on fine chemical production.

Computational study of representative reaction pathways

Regarding the selective synthesis of GVL and 1,4-PD from EL in the presence of Cs_2CO_3 and $(EtO)_3SiH$, the *in situ* formed silyl ethers **Si-1** and **Si-2** were verified to be the key intermediates (*vide supra*), respectively. In particular, the efficiency in the consecutive addition of one to three equiv. hydrides to EL seemed essential for the formation of the silyl ethers (Fig. S22†). DFT calculations were performed to examine the free energies of the dominant products involved in the reaction pathways, and the resulting energy profiles are shown in Fig. S23.† Both **Si-1** and **Si-2** were found to have lower free energies (−17.20 and −15.38 kcal mol^{-1}, respectively) than the starting material EL. These two silyl ethers with moderate stability can not only remain intact during the reaction process under mild conditions, but can also be further degraded to remove the siloxane moiety at an elevated temperature, rendering them ideal precursors of GVL and 1,4-PD. It should be noted that EL acetal derived from **Si-1** was calculated to have a higher free energy (−2.87 kcal mol^{-1}, Fig. S22†), implying that the dominant barrier toward 1,4-PD from EL was the ester hydrogenation step. This finding is consistent with the experimental results, where **Si-1** (precursor of GVL) can be rapidly and quantitatively formed in 0.5 h, while approximately 6 h are required to obtain **Si-2** (precursor of 1,4-PD).

In addition, we note that a significant difference in product distribution was observed when lactone and lactam were used as substrates with $PhSiH_3$ as the hydrogen source for reduction (Fig. S24†). In the case of a lactone (*e.g.*, GVL), a diol (1,4-PD) was likely to be obtained, while the complete reduction of lactam (*e.g.*, 1,5-dimethyl-2-pyrrolidinone (DPO)) gave cyclamine (1,2-dimethylpyrrolidine (DPI)) as the predominant product. DFT calculations demonstrated the significance of

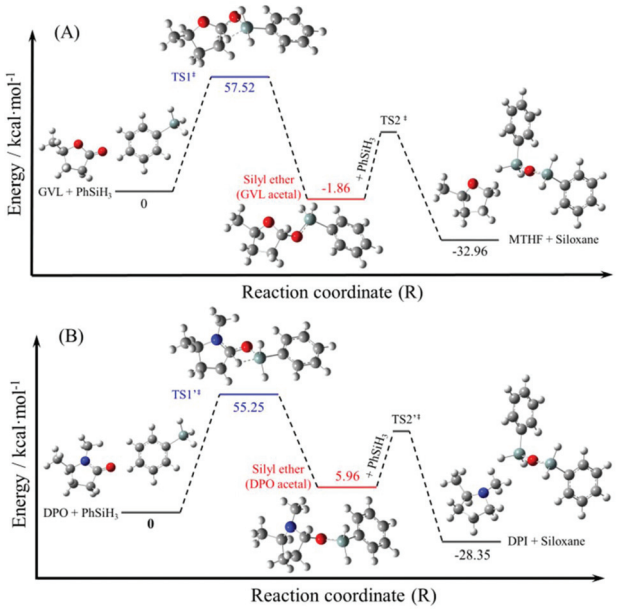

Fig. 5 DFT calculation results of silyl ether *in situ* formed from the lactone and lactam using $PhSiH_3$ as a H-donor. Energy profiles for the reduction of (A) γ-valerolactone (GVL) to 2-methyltetrahydrofuran (MTHF) and (B) 1,5-dimethyl-2-pyrrolidinone (DPO) to 1,2-dimethylpyrrolidine (DPI) *via* the corresponding silyl ethers. The optimized transition state (**TS1**) structures are shown in blue. Computational free energy values (in kcal mol^{-1}) are displayed.

the type of silyl ether formed *in situ* (*i.e.*, GVL/DPO acetals) along with its preceding optimized transition state (**TS1**) in the selectivity control (Fig. 5). The **TS1** free energy for the initial reduction of GVL was found to be slightly higher than that for the initial hydrogenation of DPO (57.52 *vs.* 55.25 kcal mol^{-1}), indicating the need for a relatively higher energy barrier to form a GVL-derived acetal: (5-methyltetrahydrofuran-2-yl)oxy phenylsilane. Moreover, the stability of this compound was higher than that of the corresponding intermediate (DPO-derived acetal), in view of their free energies (−1.86 *vs.* +5.96 kcal mol^{-1}). This finding rationalizes the difficulty in the synthesis of MTHF from GVL, which is in agreement with the experimental results. In fact, 1,4-PD was detected to be the main product from the reduction of GVL, showing that the cyclic C–O bond was more easily broken than the exocyclic bond of the GVL acetal during the hydrosilylation process, as illustrated in Fig. S24.† In contrast, the exocyclic C–O bond of the DPO-derived acetal was susceptible to cleavage, affording the cyclamine (DPI) as the principal product. The presence of competing reaction pathways dependent on the structures of *in situ* formed silyl ethers makes the product distribution controllable.

Conclusions

In summary, an economic and green catalytic system composed of Cs_2CO_3, hydrosilane and the bio-based solvent MTHF has been developed for the room-temperature reduction of dicarbonyl compounds into monohydric esters or diols in 85–99% yields using 1.5–3.5 equiv. H^-. In particular, the cyclization/lactonization of ethyl 4-hydroxypentanoate (EHP) or its silyl ether (**Si-1**) formed *in situ* from biomass-derived ethyl levulinate (EL) can take place through a facile post-treatment process, quantitatively giving the valuable platform molecule γ-valerolactone (GVL). The process exhibits a TOF value (39.2 h^{-1}) that is superior to previous results obtained using metal catalysts. By an appropriate increase of the hydrosilane dosage and by an extension of the reaction time, 1,4-pentanediol (1,4-PD) instead of GVL can become the dominant product (up to 95% yield), while cyclic ether formation (self-etherification) or monohydric alcohol formation (over-hydrogenation) is absent. The *in situ* formation of silyl ether is most likely responsible for the pronounced performance and selectivity toward different types of carbonyl species, as demonstrated by *in situ* NMR and computational studies. Despite requiring longer reaction times, a variety of monohydric amides and hydroxylamines can be synthesized from the corresponding dicarboxides, while the other concurrent unsaturated species remain intact. The high selectivity and benign reaction conditions make our catalytic system a promising alternative to precious metal catalysts in the specific reduction of carbonyl groups. In addition, the concept of *in situ* generating a labile silyl ether between the reactant and hydride bears promise in the switchable reduction or transformation of specific species from multi-functional groups in both biomass feedstock and relevant molecules.

Experimental

Materials

Tetrahydrofuran-d_8 (99.5 atom % D), methanol-d_4 (99.8 atom % D), diphenylsilane-d_2 (97 atom % D), and Amberlyst-15 (hydrogen ion form, wet) were purchased from Shanghai Sigma-Aldrich Trading Co. Ltd. Cesium carbonate (Cs_2CO_3, 99%), 2-methyltetrahydrofuran (MTHF, 99%), 18-crown-6 (99%), triethoxysilane [$(EtO)_3SiH$, 95%], phenylsilane ($PhSiH_3$, 97%), ethyl levulinate (EL, 99%), γ-valerolactone (GVL, 98%), 1,4-pentanediol (1,4-PD, 99%), naphthalene (99%), and xylene (99%) were purchased from Beijing InnoChem Science & Technology Co., Ltd.

Reduction of multi-unsaturated carbonyl compounds

All the reduction reactions were carried out in Ace pressure tubes (10 mL). In a typical procedure, 1 mmol carbonyl compound, 1–5.5 equiv. H^- of hydrosilane, 5 mol% Cs_2CO_3, and 2 mL MTHF were added into the tube. After stirring (500 rpm) at room temperature (25 °C) for a specific reaction time, 2 mL ethanol was added into the reaction mixture and stirring continued at 80 °C for another 2 h. The resulting solution was collected and subjected to product analysis.

Product analysis

Dominant products were identified by GC-MS (Agilent 6890N combined with 5973 MS), whereas the quantification of liquid

products was performed using a GC system (Agilent 7890B) fitted with a flame ionization detector (FID) and a HP-5 column (30 m × 0.320 mm × 0.25 μm) using naphthalene as an internal standard and referring to standard curves. The content of formate was determined by ^{1}H NMR using xylene as an internal standard.

NMR spectroscopic study

^{1}H, ^{13}C and 2D ^{1}H–^{13}C HSQC NMR spectra of the liquid mixtures were obtained with normal hydrosilanes in deuterated solvents (typically, MTHF-d_{10}) or in protonated solvents containing 5% DMSO-d_6 as a lock substance on a Bruker Avance III 800 MHz spectrometer equipped with a TCI cryoprobe. The *ex situ* samples of reaction progress were obtained by quenching reactions with methanol-d_4 at indicated times. For the isotope-labeling study, ^{1}H, ^{13}C, DEPT-135 and ^{1}H–^{13}C HSQC NMR spectra of the reaction mixtures, which were obtained using deuterium reagents (diphenylsilane-d_2 and THF-d_8 with or without CD_3OD post-treatment), were recorded on a JEOL-ECX 500 NMR spectrometer.

Conflicts of interest

There are no conflicts to declare.

Acknowledgements

This work is financially supported by the National Natural Science Foundation of China (21576059 and 21666008), Fok Ying-Tong Education Foundation (161030), Guizhou Science & Technology Foundation ([2018]1037 and [2017]5788), and Key Technologies R&D Program of China (2014BAD23B01). We acknowledge the NMR center DTU (Denmark) for recording NMR spectra, and Institute of Chemistry (CAS) for DFT calculations. S. S. thanks the Department of Biotechnology (Government of India) New Delhi, India for support.

Notes and references

1 (*a*) D. Wang and D. Astruc, *Chem. Rev.*, 2015, **115**, 6621–6686; (*b*) J. H. Xie, S. F. Zhu and Q. L. Zhou, *Chem. Rev.*, 2011, **111**, 1713–1760; (*c*) J. Pritchard, G. A. Filonenko, R. van Putten, E. J. M. Hensen and E. A. Pidko, *Chem. Soc. Rev.*, 2015, **44**, 3808–3833.

2 (*a*) R. M. Bullock, *Science*, 2013, **342**, 1054–1055; (*b*) A. Corma and P. Serna, *Science*, 2006, **313**, 332–334; (*c*) P. Ryabchuk, G. Agostini, M. M. Pohl, H. Lund, A. Agapova, H. Junge, K. Junge and M. Beller, *Sci. Adv.*, 2018, **4**, eaat0761.

3 (*a*) K. Manna, T. Zhang, M. Carboni, C. W. Abney and W. Lin, *J. Am. Chem. Soc.*, 2014, **136**, 13182–13185; (*b*) H. Li, Z. Fang, R. L. Smith and S. Yang, *Prog. Energy Combust. Sci.*, 2016, **55**, 98–194; (*c*) M. Naruto and S. Saito, *Nat. Commun.*, 2015, **6**, 8140; (*d*) T. J. Korstanje, J. I. van der Vlugt, C. J. Elsevier and B. de Bruin, *Science*, 2015, **350**, 298–302; (*e*) K. Yuan, T. Song, D. Wang, X. Zhang, X. Gao, Y. Zou, H. Dong, Z. Tang and W. Hu, *Angew. Chem., Int. Ed.*, 2018, **57**, 5708–5713; (*f*) R. C. Cammarota and C. C. Lu, *J. Am. Chem. Soc.*, 2015, **137**, 12486–12489; (*g*) L. Wang, E. Guan, J. Zhang, J. Yang, Y. Zhu, Y. Han, M. Yang, C. Cen, G. Fu, B. C. Gates and F. S. Xiao, *Nat. Commun.*, 2018, **9**, 1362.

4 (*a*) C. Pilar Jiménez-Gómez, J. A. Cecilia, D. Durán-Martín, R. Moreno-Tost, J. Santamaría-González, J. Mérida-Robles, R. Mariscal and P. Maireles-Torres, *J. Catal.*, 2016, **336**, 107–115; (*b*) G. W. Huber, J. N. Chheda, C. J. Barrett and J. A. Dumesic, *Science*, 2005, **308**, 1446–1450; (*c*) C. Zhao, Y. Kou, A. A. Lemonidou, X. Li and J. A. Lercher, *Angew. Chem., Int. Ed.*, 2009, **48**, 3987–3990.

5 (*a*) Q. Meng, M. Hou, H. Liu, J. Song and B. Han, *Nat. Commun.*, 2017, **8**, 14190; (*b*) M. Tamura, N. Yuasa, J. Cao, Y. Nakagawa and K. Tomishige, *Angew. Chem., Int. Ed.*, 2018, **57**, 8058–8062.

6 (*a*) W. Liu, Y. Jiang, K. H. Dostert, C. P. O'Brien, W. Riedel, A. Savara, S. Schauermann and A. Tkatchenko, *Sci. Adv.*, 2017, **3**, e1700939; (*b*) Y. Zhu, H. Qian, B. A. Drake and R. Jin, *Angew. Chem., Int. Ed.*, 2010, **49**, 1295–1298.

7 (*a*) C. O. Tuck, E. Pérez1, I. T. Horváth, R. A. Sheldon and M. Poliakoff, *Science*, 2012, **337**, 695–699; (*b*) Y. S. Jang, B. Kim, J. H. Shin, Y. J. Choi, S. Choi, C. W. Song, J. Lee, H. G. Park and S. Y. Lee, *Biotechnol. Bioeng.*, 2012, **109**, 2437–2459; (*c*) H. Li, A. Riisager, S. Saravanamurugan, A. Pandey, R. S. Sangwan, S. Yang and R. Luque, *ACS Catal.*, 2018, **8**, 148–187; (*d*) H. Li and R. L. Smith, *Nat. Catal.*, 2018, **1**, 176–177.

8 (*a*) Y. Román-Leshkov, C. J. Barrett, Z. Y. Liu and J. A. Dumesic, *Nature*, 2007, **447**, 982–985; (*b*) J. N. Chheda, G. W. Huber and J. A. Dumesic, *Angew. Chem., Int. Ed.*, 2007, **46**, 7164–7183; (*c*) D. M. Alonso, S. G. Wettstein and J. A. Dumesic, *Green Chem.*, 2013, **15**, 584–595.

9 (*a*) W. Deng, Y. Wang and N. Yan, *Curr. Opin. Green Sustain. Chem.*, 2016, **2**, 54–58; (*b*) H. Li, Z. Fang, J. Luo and S. Yang, *Appl. Catal., B*, 2017, **200**, 182–191.

10 (*a*) Z. Zhang, *ChemSusChem*, 2016, **9**, 156–171; (*b*) B. Banerjee, R. Singuru, S. K. Kundu, K. Dhanalaxmi, L. Bai, Y. Zhao, B. M. Reddy, A. Bhaumik and J. Mondal, *Catal. Sci. Technol.*, 2016, **6**, 5102–5115; (*c*) S. Pendem, I. Mondal, A. Shrotri, B. S. Rao, N. Lingaiah and J. Mondal, *Sustainable Energy Fuels*, 2018, **2**, 1516–1529; (*d*) K. Dhanalaxmi, R. Singuru, S. Mondal, L. Bai, B. M. Reddy, A. Bhaumik and J. Mondal, *ACS Sustainable Chem. Eng.*, 2017, **5**, 1033–1045; (*e*) D. Ren, X. Wan, F. Jin, Z. Song, Y. Liu and Z. Huo, *Green Chem.*, 2016, **18**, 5999–6003; (*f*) T. Mizugaki, Y. Nagatsu, K. Togo, Z. Maeno, T. Mitsudome, K. Jitsukawa and K. Kaneda, *Green Chem.*, 2015, **17**, 5136–5139; (*g*) J. Cui, J. Tan, Y. Zhu and F. Cheng, *ChemSusChem*, 2018, **11**, 1316–1320; (*h*) S. C. Patankar and G. D. Yadav, *ACS Sustainable Chem. Eng.*, 2015, **3**, 2619–2630.

11 (*a*) S. G. Wettstein, D. M. Alonso, Y. Chong and J. A. Dumesic, *Energy Environ. Sci.*, 2012, **5**, 8199–8203; (*b*) W. Luo, M. Sankar, A. M. Beale, Q. He, C. J. Kiely,

P. C. A. Bruijnincx and B. M. Weckhuysen, *Nat. Commun.*, 2015, **6**, 6540; (*c*) A. Primo, P. Concepción and A. Corma, *Chem. Commun.*, 2011, **47**, 3613–3615; (*d*) T. Mizugaki, Y. Nagatsu, K. Togo, Z. Maeno, T. Mitsudome, K. Jitsukawa and K. Kaneda, *Green Chem.*, 2015, **17**, 5136–5139; (*e*) D. Addis, S. Das, K. Junge and M. Beller, *Angew. Chem., Int. Ed.*, 2011, **50**, 6004–6011; (*f*) A. Volkov, K. P. J. Gustafson, C. W. Tai, O. Verho, J. E. Bäckvall and H. Adolfsson, *Angew. Chem., Int. Ed.*, 2015, **54**, 5122–5126; (*g*) H. Li, W. Zhao and Z. Fang, *Appl. Catal., B*, 2017, **215**, 18–27.

12 F. Lehmann, *Synlett*, 2004, 2447–2448.

13 (*a*) X. Y. Li, R. Shang, M. C. Fu and Y. Fu, *Green Chem.*, 2015, **17**, 2790–2793; (*b*) W. Zhao, T. Yang, H. Li, W. Wu, Z. Wang, C. Fang, S. Saravanamurugan and S. Yang, *ACS Sustainable Chem. Eng.*, 2017, **5**, 9640–9644; (*c*) X. F. Liu, C. Qiao, X. Y. Li and L. N. He, *Green Chem.*, 2017, **19**, 1726–1731; (*d*) H. Li, W. Zhao, A. Riisager, S. Saravanamurugan, Z. Wang, Z. Fang and S. Yang, *Green Chem.*, 2017, **19**, 2101–2106; (*e*) C. Wu, X. Luo, H. Zhang, X. Liu, G. Ji, Z. Liu and Z. Liu, *Green Chem.*, 2017, **19**, 3525–3529; (*f*) H. Li, W. Zhao, S. Saravanamurugan, W. Dai, J. He, S. Meier, S. Yang and A. Riisager, *Chem. Commun.*, 2018, **1**, 32; (*g*) C. Xu, B. Huang, T. Yan and M. Cai, *Green Chem.*, 2018, **20**, 391–397; (*h*) R. A. Pramudita and K. Motokura, *Green Chem.*, 2018, **20**, 4834–4843.

14 (*a*) T. Mizugaki, Y. Nagatsu, K. Togo, Z. Maeno, T. Mitsudome, K. Jitsukawa and K. Kaneda, *Green Chem.*, 2015, **17**, 5136–5139; (*b*) T. Mizugaki, K. Togo, Z. Maeno, T. Mitsudome, K. Jitsukawa and K. Kaneda, *ACS Sustainable Chem. Eng.*, 2016, **4**, 682–685; (*c*) D. Ren, X. Wan, F. Jin, Z. Song, Y. Liu and Z. Huo, *Green Chem.*, 2016, **18**, 5999–6003.

15 (*a*) K. K. Senapati, Polymethylhydrosiloxane (PMHS), *Synlett*, 2005, 1960–1961; (*b*) D. B. Nale and B. M. Bhanage, *Green Chem.*, 2015, **17**, 2480–2486; (*c*) J. A. Caetano and A. C. Fernandes, *Green Chem.*, 2018, **20**, 2494–2498.

16 M. Chia, Y. J. Pagán-Torres, D. Hibbitts, Q. Tan, H. N. Pham, A. K. Datye, M. Neurock, R. J. Davis and J. A. Dumesic, *J. Am. Chem. Soc.*, 2011, **133**, 12675–12689.

17 S. Wang, H. Huang, C. Bruneau and C. Fischmeister, *ChemSusChem*, 2017, **10**, 4150–4154.

18 G. Gao, P. Sun, Y. Li, F. Wang, Z. Zhao, Y. Qin and F. Li, *ACS Catal.*, 2017, **7**, 4927–4935.

19 (*a*) J. R. Cabrero-Antonino, E. Alberico, K. Junge, H. Junge and M. Beller, *Chem. Sci.*, 2016, **7**, 3432–3442; (*b*) N. M. Rezayee, D. C. Samblanet and M. S. Sanford, *ACS Catal.*, 2016, **6**, 6377–6383; (*c*) V. Papa, J. R. Cabrero-Antonino, E. Alberico, A. Spanneberg, K. Junge, H. Junge and M. Beller, *Chem. Sci.*, 2017, **8**, 3576–3585.

20 (*a*) J. M. Woodley, *Trends Biotechnol.*, 2008, **26**, 321–327; (*b*) N. L. Lampland, M. Hovey, D. Mukherjee and A. D. Sadow, *ACS Catal.*, 2015, **5**, 4219–4226; (*c*) Y. Q. Zou, S. Chakraborty, A. Nerush, D. Oren, Y. Diskin-Posner, Y. Ben-David and D. Milstein, *ACS Catal.*, 2018, **8**, 8014–8019.